Developmental Biology **230,** 177–188 (2001)
doi:10.1006/dbio.2000.0134, available online at http://www.idealibrary.com on IDEAL®

TBX5 Transcription Factor Regulates Cell Proliferation during Cardiogenesis

Cathy J. Hatcher,*,†,[1] Min-Su Kim,*,†,[1] Caroline S. Mah,*,†,[1] Marsha M. Goldstein,‡ Benjamin Wong,* Takashi Mikawa,† and Craig T. Basson*,†,[2]

**Molecular Cardiology Laboratory, Cardiology Division, Department of Medicine, Weill Medical College of Cornell University, 525 E. 68th Street, New York, New York 10021; †Department of Cell Biology, Weill Medical College of Cornell University, 1300 York Avenue, New York, New York 10021; and ‡Division of Anatomic Pathology, Quest Diagnostics, Teterboro, New Jersey 07608*

Mutations in human *TBX5*, a member of the T-box transcription factor gene family, cause congenital cardiac septation defects and isomerism in autosomal dominant Holt–Oram syndrome. To determine the cellular function of TBX5 in cardiogenesis, we overexpressed wild-type and mutant human TBX5 isoforms *in vitro* and *in vivo*. TBX5 inhibited cell proliferation of D17 canine osteosarcoma cells and MEQC quail cardiomyocyte-like cells *in vitro*. Mutagenesis of the 5′ end of the T-box but not the 3′ end of the T-box abolished this effect. Overexpression of TBX5 in embryonic chick hearts showed that TBX5 inhibits myocardial growth and trabeculation. TBX5 effects *in vivo* were abolished by Gly80Arg missense mutation of the 5′ end of the T-box. PCNA analysis in transgenic chick hearts revealed that TBX5 overexpression does suppress embryonic cardiomyocyte proliferation *in vivo*. Inhibitory effects of TBX5 on cardiomyocyte proliferation include a noncell autonomous process *in vitro* and *in vivo*. TBX5 inhibited proliferation of both nontransgenic cells cocultured with transgenic cells *in vitro* and nontransgenic cardiomyocytes in transgenic chick hearts with mosaic expression of TBX5 *in vivo*. Immunohistochemical studies of human embryonic tissues, including hearts, also demonstrated that TBX5 expression is inversely related to cellular proliferation. We propose that TBX5 can act as a cellular arrest signal during vertebrate cardiogenesis and thereby participate in modulation of cardiac growth and development.

INTRODUCTION

TBX5, a T-box transcription factor (Chapman *et al.*, 1996), plays a critical role in vertebrate cardiac morphogenesis. Mutations in human *TBX5* cause Holt–Oram syndrome, an autosomal dominant disorder characterized by cardiac malformation, including defects in septation and isomerism, and upper limb deformity (Basson *et al.*, 1997, 1999; Li *et al.*, 1997). Although alterations in human TBX5 gene dose, either haploinsufficiency or TBX5 overexpression via gene duplication (Melnyk *et al.*, 1981; McCorquodale *et al.*, 1986; Dixon *et al.*, 1993; Hatcher and Basson, 2000), severely perturb both heart and limb development, missense mutations in TBX5 affect the heart and limb to varying degrees (Basson *et al.*, 1999; Yang *et al.*, 2000). Modification of either end of the T-box alters DNA binding *in vitro* (Kispert and Herrmann, 1993; Herrmann and Kispert, 1994). In humans, missense mutations which disrupt the 5′ end of the T-box have more severe cardiac effects than missense mutations at the 3′ end of the T-box (Basson *et al.*, 1999; Yang *et al.*, 2000). These missense mutations map to domains at the 5′ and 3′ ends of the T-box that have been predicted by X-ray crystallographic studies to include binding sites for the major and minor grooves of target DNA, respectively (Müller and Herrmann, 1997; Basson *et al.*, 1999).

Little is known about the specific cellular activities regulated by TBX5 during cardiogenesis. Others (Rodriguez-Esteban *et al.*, 1999; Takeuchi *et al.*, 1999) have used data

[1] These authors contributed equally to this manuscript.

[2] To whom correspondence should be addressed at Molecular Cardiology Laboratory, Cardiology Division, Dept. of Medicine, Weill Medical College of Cornell University, 525 E. 68th Street, New York, NY 10021. Fax: (212) 746-2222. E-mail: ctbasson@med.cornell.edu.

0012-1606/01 $35.00

from investigation of overexpression of Tbx5 in the chick limb to demonstrate that Tbx5 contributes to the establishment of limb identity during embryogenesis. Rodriguez-Esteban *et al.* (1999) further hypothesized that chick Tbx5 might interact with growth factors to modify cell proliferation during limb outgrowth and specification. A similar role for Tbx5 has been hypothesized during newt limb regeneration and specification [Simon *et al.* (1997)]. Horb and Thomsen (1999) demonstrated that Tbx5 was essential for normal cardiac morphogenesis in Xenopus, and recently, Liberatore *et al.* (2000) showed that overexpression of TBX5 in the ventricles during mouse cardiogenesis resulted in abnormal chamber specification and noted that their findings could be consistent with altered cell proliferation within the myocardium. In the current studies, we now demonstrate that ectopic overexpression of human TBX5 inhibits cell proliferation *in vitro* and during chick cardiogenesis *in vivo*. This TBX5 activity is no longer evident if the glycine at position 80 is mutated to arginine. Immunohistochemistry reveals that TBX5 localization is inversely related to localization of nuclear markers of cell proliferation during human cardiogenesis. We, therefore, propose that TBX5 acts as a cellular arrest signal during vertebrate cardiac development.

MATERIALS AND METHODS

Site-Directed Mutagenesis of Human TBX5

The *Gly80Arg–TBX5* mutant cDNA was generated by PCR with the QuikChange Site-Directed Mutagenesis kit (Stratagene) per the instructions of the manufacturer. PCR-based mutagenesis of wild-type *TBX5.3* cDNA in pBSIIKS (−) plasmid (Basson *et al.*, 1997, 1999) was performed with two synthetic oligonucleotide primers (5′-CATAACCAAGGCTAGAAGGCGGATGTTTC-3′ and 5′-GAAACATCCGCCTTCTAGCCTTGGTTATG-3′) containing the G238A transition mutation (mutated bases are underlined in primer sequences above; Basson *et al.*, 1999). Δ*Asn198FSter–TBX5* was a naturally occurring mutation in the *TBX5.2* clone (Basson *et al.*, 1997). Both mutations were confirmed by automated sequencing on an ABI 377 sequencer.

Retroviral TBX5 Constructs

The CXIZ retrovirus used in the present study is a replication-defective variant of the avian spleen necrosis virus (Mikawa, 1995; Takebayashi-Suzuki *et al.*, 2000). Construction of the viral vectors and propagation of the recombinant virus have been previously described (Mikawa *et al.*, 1992b; Mikawa, 1995; Mima *et al.*, 1995; Takebayashi-Suzuki *et al.*, 2000). A 1935-bp fragment containing the entire TBX5 coding sequence (exons 2–9) was excised from wild-type or mutant *TBX5.3* or *TBX5.2* cDNA in pBSIIKS (−) plasmid with *Sac*II and *Stu*I. Linker adaptor pairs (5′-GGGAGCGCGCGTAATACGACTCACTATAGAACCGC-3′/5′-GGTTCTATAGTGAGTCGTATTACGCGCGCTCCC-3′; 5′-GAAATCACTCCCAATTAACGCGCGAAT-3′/5′-CTAGATTCGCGCGTTAATTGGGAGTGATTTC-3′) were ligated to the 5′ and 3′ ends of the *TBX5* inserts, and inserts were then were subcloned into *Sma*I and *Xba*I restriction enzyme sites in the pCXIZ plasmid. *TBX5* coding sequences were thereby inserted into pCXIZ between the 5′LTR and an internal ribosome entry sequence (IRES) derived from the 5′ untranslated region of the encephalomyocardi-

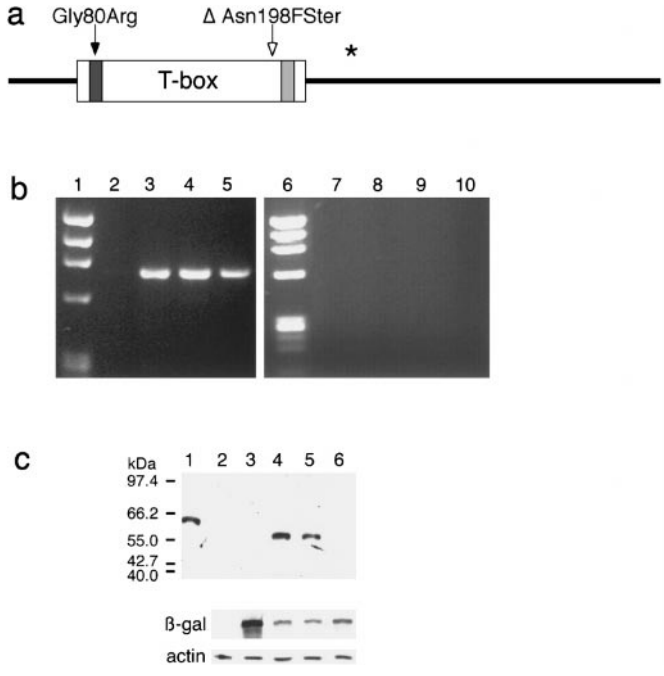

FIG. 1. Retroviral overexpression of wild-type and mutant TBX5. (a) Schematic of TBX5 cDNA showing the T-box DNA binding domain. X-ray crystallographic studies (Müller and Herrmann, 1997) have predicted disparate binding sites for target DNA major groove (dark gray) and for target DNA minor groove (light gray). These sites are shown relative to the positions of the Gly80Arg missense mutation (closed arrow), the ΔASN198FSter truncation mutation (open arrow), and the anti-TBX5 antibody recognition epitope (*). (b) RT-PCR analysis of D17 cells infected with TBX5-CXIZ viruses demonstrates transcription of the TBX5 transgene. A 780-bp portion of TBX5 cDNA is amplified from D17s infected with wt-TBX5-CXIZ (lane 3), Gly80Arg-TBX5-CXIZ (lane 4), and ΔAsn198FSter-TBX5-CXIZ (lane 5), but not from D17s infected with the CXIZ retrovirus alone (lane 2). rt-PCR experimental controls (lanes 6–10) demonstrate no genomic DNA contamination was present in total cellular RNA isolated from D17s infected with CXIZ retrovirus alone (lane 7), wt-TBX5-CXIZ (lane 8), Gly80Arg-TBX5-CXIZ (lane 9), or ΔAsn198FSter-0TBX5-CXIZ (lane 10). DNA size marker, ϕX174/*Hae*III, is shown in lanes 1 and 6. (c) Western blot analysis with anti-TBX5 antibody demonstrates specific synthesis of 58 kDa rhTBX5 protein by D17s infected with TBX5-CXIZ retroviruses. (1) Recombinant 62 kDa calmodulin binding protein-TBX5 fusion protein (Hatcher *et al.*, 2000); (2) D17 cells; (3) CXIZ-infected D17s; (4) wt-TBX5-CXIZ infected D17s; (5) Gly80Arg-TBX5-CXIZ infected D17s; (6) ΔAsn198FSter-TBX5-CXIZ infected D17s. Note that the mutant ΔAsn198FSter-TBX5 protein is not recognized by anti-TBX5 since this mutant isoform is truncated prior to the antibody recognition site (see a). Shown below the Western blot analysis of infected D17s for rhTBX5 synthesis are Western blot analyses of infected D17s for recombinant β-galactosidase (encoded by CXIZ retroviruses) and for native actin.

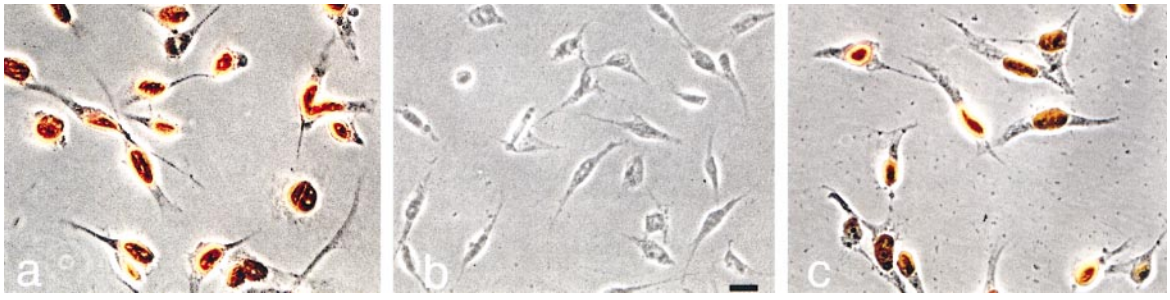

FIG. 2. Immunohistochemical detection of overexpression of wild-type and mutant TBX5 in cultured cells. Immunohistochemistry of D17s infected with wt-TBX5-CXIZ (a) or Gly80Arg-TBX5-CXIZ (c) for rhTBX5 demonstrates translocation of the recombinant TBX5 transcription factor to the cell nuclei, but not in D17s infected with the CXIZ retrovirus alone (panel b). (Bar = 10 μm.)

tis virus genome. Because the IRES is upstream from the bacterial *lacZ* gene, both the subcloned TBX5 transgene and the *lacZ* gene are expressed from a dicistronic mRNA. Cotranslation of the transgene and β-galactosidase from the dicistronic mRNA in daughter populations from infected cells has been previously demonstrated both in tissue culture and in chick embryos (Mikawa *et al.*, 1992b, Mima *et al.*, 1995). Automated sequencing on an ABI 377 sequencer of all pCXIZ plasmids confirmed the appropriate TBX5 isoform sequence. Viruses were propagated and titers assayed per published protocols (Mikawa *et al.*, 1992b; Takebayashi-Suzuki *et al.*, 2000). We obtained titers of approximately 10^6 virions/ml for all CXIZ viruses in the supernatant of each clone of virus-producing cells.

Cell Proliferation

Over a 48-h period, 2×10^5 D17 canine osteosarcoma cells or MEQC cells (a *myc*-transformed avian cardiomyocyte-like cell line, gift of T. Jaffredo and A. Conrad; Jaffredo *et al.*, 1991) were infected with 5×10^4 virions of modified CXIZ virus encoding wild-type or mutant (Gly80Arg or ΔAsn198FSter) TBX5 isoforms or unmodified CXIZ control virus in the presence of 10 μg/ml polybrene. Cells were then harvested and replated at 5×10^4 cells per 60 mm^2 dish. Cells were grown in culture for 1 to 4 days, and at multiple time points, culture dishes were fixed with 2% paraformaldehyde and stained with X-Gal (5-bromo-4-chloro-3-indolyl-β-gal) for β-galactosidase activity. The number of β-galactosidase-positive and -negative cells/16 mm^2 was determined by direct visualization via light microscopy beginning 6 h after plating.

Retroviral Infection of Chick Embryos In Ovo

Media supernatants containing CXIZ viruses encoding β-galactosidase and TBX5 isoforms or, for control experiments, β-galactosidase alone were collected and concentrated by ultracentrifugation as previously described (Mikawa *et al.*, 1992b). Fertilized chick eggs obtained from an outbred flock were incubated at 37.5°C in a humidified atmosphere until Hamburger–Hamilton (HH) stages 17–18 (Hamburger and Hamilton, 1951). A 5–10 mm diameter window was opened in the shell at the blunt end of the egg and the underlying shell membrane was removed. Ten to 100 viral particles in 1–5 nl solution (DMEM with 7% FBS) containing 100 μg/ml polybrene were pressure-injected into the myocardium of the beating tubular heart *in ovo* as previously described (Mima *et al.*, 1995). Eggs were resealed with parafilm and incubated until embryos were sacrificed at E15. Six to 16 embryos were injected with each virus. *In ovo* infection efficiency was determined by fixing the hearts with 2% paraformaldehyde and staining overnight for β-galactosidase activity with X-Gal. CXIZ-mediated gene expression has been previously demonstrated (Wei and Mikawa, 2000) to begin within 7–9 h of retroviral microinjection.

Immunohistochemistry of Human and Chick Tissues

Human cardiac tissue was obtained as waste surgical pathology material from therapeutic abortions of ten 10–15 gestational week

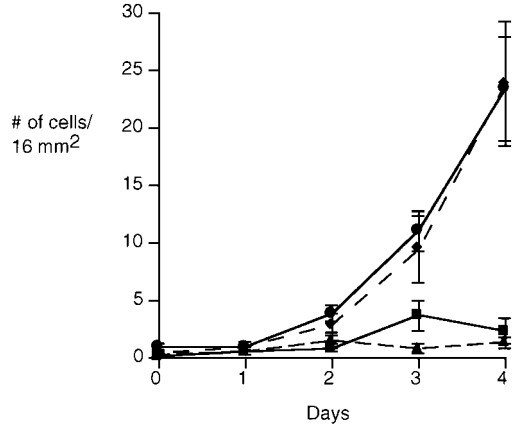

FIG. 3. Effect of overexpression of wild-type and mutant TBX5 isoforms on D17 proliferation. D17 cells were infected with wt-TBX5-CXIZ (solid line, ■), CXIZ alone (solid line, ●), or mutant TBX5-CXIZ isoforms (dashed lines), Gly80Arg-TBX5-CXIZ (large dashes, ◆) or ΔAsn198FSter-TBX5-CXIZ (small dashes, ▲). The number of infected D17 cells (identified by histochemical staining for β-galactosidase activity) per 16 mm^2 was determined by direct visualization at daily time points over 4 days. Wt-TBX5 overexpression inhibits cell proliferation as does overexpression of ΔAsn198FSter-TBX5. However, the Gly80Arg mutation blocks TBX5-mediated inhibition of D17 proliferation.

embryos with informed consent and approval of the Cornell Committee on Human Rights on Research (Hatcher *et al.*, 2000). Embryonic chick cardiac tissues were obtained at E15. Tissues were paraformaldehyde-fixed and paraffin-embedded, or they were flash frozen and embedded in tissue freezing medium (Fisher) for cryosectioning.

Five micron paraffin sections were either pretreated with antigen retrieval (Biogenex) and incubated with affinity-purified anti-TBX5 (Hatcher *et al.*, 2000) or anti-Ki67 (Dako) or were incubated directly without pretreatment with anti-β-galactosidase (Biogenesis), or anti-PCNA (Dako). Bound primary antibody was detected with secondary antibody conjugated to horseradish peroxidase or alkaline phosphatase (LSAB2, Dako). Double immunostaining was performed with the Envision Double Staining Kit (Dako) and Vector Red alkaline phosphatase substrate (Vector).

Ten micron frozen sections were air dried and then incubated with primary antibodies: anti-atrial myosin heavy chain (AMHC1, gift of Dr. Robert Gourdie, Medical College of South Carolina; Sanders *et al.*, 1984), anti-actin (Sigma), or affinity-purified anti-TBX5. Bound primary antibody was detected with secondary antibody conjugated to horseradish peroxidase (LSAB2, Dako). To detect apoptotic cells, frozen sections were fixed in paraformaldehyde and then analyzed with a modified TUNEL assay, the DeadEnd Colorimetric Apoptosis Detection System (Promega), per the instructions of the manufacturer. In brief, sections were permeabilized with proteinase K, incubated with biotinylated nucleotides and terminal deoxynucleotidyl transferase, washed in 2× SSC, quenched with 0.3% hydrogen peroxide, incubated with streptavidin–horseradish peroxidase, and product visualized with diaminobenzidine chromogen. Control sections were treated with DNase after permeabilization.

Immunohistochemistry of Cultured Cells

Cells were fixed in McClean's fixative (10 mM $NaIO_4$, 750 mM lysine, 37.5 mM $NaPO_4$, 2% paraformaldehyde) for 30 min on ice and then permeabilized with 0.2% Triton in PBS for 20 min on ice. Overnight blocking for nonspecific binding sites was performed at 4°C in 3% bovine serum albumin/PBS. Further immunohistochemical staining was performed with affinity-purified anti-TBX5 and the LSAB2 peroxidase system (Dako) per the instructions of the manufacturer. The DeadEnd Colorimetric Apoptosis Detection System (Promega) was used for detection of apoptotic cell death in cultured cells in the same manner as for detection in tissue sections except cells were permeabilized with Triton X-100 instead of proteinase K.

RT-PCR

Total RNA was isolated from cell cultures using the RNeasy Mini Kit (Qiagen) and DNase-treated. To analyze rhTBX5 mRNA expression, 500 ng RNA was reverse transcribed and subsequently amplified by the Access RT-PCR System (Promega) with primers TBX5ATGF (5′-ATGGCCGACGCAGACGAGGGC-3′) and TBX5-AGGR (5′-AGGTCTGGTGCTGGAACATT-3′). To ensure that genomic DNA was not contaminating our total RNA sample and, thus amplified as a product of the PCR reaction, we performed parallel control rt-PCR experiments in which rt-PCR of total RNA was performed in the presence of DNA polymerase alone without reverse transcriptase. Amplified material was purified (Qiaquick, Qiagen) and a subsequent nested PCR amplification [94°C × 2 min followed by (94°C × 30 s, 58°C × 30 s, 72°C × 1 min) × 35 cycles] was performed with primers 29exF (5′-CGGGCAAAGCTGAGC-3′) and ex9R (5′-GCTGGCATACATGCAAGCTTGCCGC-3′) to amplify a 780-bp product. PCR products were analyzed on 2% agarose gels.

SDS–PAGE and Western Blotting

Cultured cells were solubilized in 2% SDS. Lysate corresponding to 50 μg of total protein was electrophoresed on a 7.5% acrylamide denaturing gel and transferred to PVDF membrane. Protein expression was detected by Western blotting with primary antibody: 0.2 μg/ml affinity-purified anti-TBX5, 1 μg/ml anti-β-galactosidase (ICN), or 0.7 μg/ml anti-actin (Sigma). Bound primary antibody was detected by ECL (Amersham).

RESULTS

In Vitro Analysis of TBX5 Activity

To study TBX5 effects on cell proliferation *in vitro*, human TBX5 isoforms were expressed in D17 canine osteosarcoma cells; canine osteosarcoma cells have previously been used to model aspects of osteoblast differentiation (Mealy *et al.*, 1998; Shoieb *et al.*, 1998). D17 cells were infected with CXIZ retroviruses (Mikawa *et al.*, 1992b; Takebayashi-Suzuki *et al.*, 2000) encoding β-galactosidase and wild-type (wt) or mutant (Gly80Arg and ΔASN198FSter) TBX5 isoforms (Fig. 1a). The Gly80Arg mutation alters the 5′ end of the T-box at a putative binding domain for target DNA's major groove (Herrmann and Kispert, 1994; Müller and Herrmann, 1997; Basson *et al.*, 1999). In contrast, the ΔASN198FSter mutation does not modify this domain but yields a truncated protein that lacks the 3′ end of the T-box including a putative T-box binding domain for target DNA's minor groove (Kispert and Herrmann, 1993; Herrmann and Kispert, 1994; Kispert *et al.*, 1995; Müller and Herrmann, 1997; Li *et al.*, 1997; Basson *et al.*, 1999). rt-PCR and Western blot analyses (Hatcher *et al.*, 2000) of infected D17s (Figs. 1b and 1c) confirmed expression of rhTBX5, and immunohistochemistry demonstrated localization to the cell nucleus (Fig. 2).

Quantification of cell proliferation (Fig. 3) revealed that wt-TBX5-CXIZ-infected D17s proliferated more slowly than D17s infected with CXIZ alone. Similar inhibition of D17 proliferation results from infection with ΔASN198FSter-TBX5-CXIZ but not Gly80Arg-TBX5-CXIZ. Changes in cell number were not a result of altered cell survival, since no induction of apoptosis was seen in the presence or absence of any TBX5 isoform.

To determine if TBX5-mediated inhibition of cell proliferation was cell autonomous, we assessed the proliferation rates of uninfected D17 cells cocultured with D17s infected with TBX5 retroviruses. We observed that after 4 days of culture, uninfected D17s cocultured with wt-TBX5-CXIZ-D17s exhibited a 32% reduction ($P < 0.01$) in cell number

compared with D17s cocultured with control CXIZ-D17s. D17s cocultured with Gly80Arg-TBX5-CXIZ-D17s exhibited normal proliferation while those cocultured with ΔASN198FSter-TBX5-CXIZ-D17s exhibited a 25% reduction ($P < 0.01$) in cell number compared with controls. Thus, we concluded that TBX5 inhibition of D17 proliferation was not cell autonomous.

Because humans heterozygous for the Gly80Arg TBX5 mutation exhibit severe cardiac manifestations of Holt–Oram syndrome, and this mutation abrogates TBX5 ability to inhibit D17 cell proliferation, we hypothesized that TBX5 might inhibit cardiomyocyte proliferation. As an initial *in vitro* test of this hypothesis, we assayed the effects of TBX5 overexpression on MEQC proliferation just as we had with D17 cells. Qualitatively similar effects were seen by TBX5 isoform overexpression on MEQCs as on D17s. By 3 days of culture, MEQCs infected with wt-TBX5-CXIZ or ΔASN198FSter-TBX5-CXIZ exhibited 58 and 52% reductions in cell number, respectively, compared with CXIZ infected MEQCs ($P < 0.01$). No significant effect on MEQC proliferation resulted from infection with Gly80Arg-TBX5-CXIZ. TBX5 inhibition of MEQC proliferation, similar to its inhibition of D17 proliferation, was not cell autonomous. Uninfected MEQCs cocultured for 3 days with wt-TBX5-CXIZ or ΔASN198FSter-TBX5-CXIZ exhibited 30 and 57% reductions in cell number, respectively, compared with those cocultured with CXIZ-infected MEQCs ($P < 0.01$).

In Vivo Analysis of TBX5 Activity during Chick Cardiogenesis

Because transformed cell lines have a limited capacity to model physiologic cardiomyocyte behavior *in vivo,* we elected to directly explore consequences of TBX5 overexpression *in vivo* in embryonic chick hearts. TBX5-CXIZ was microinjected into HH stage 17–18 chick heart myocardium (Hamburger and Hamilton, 1951; Mikawa *et al.,* 1992b; Mima *et al.,* 1995; Takebayashi-Suzuki *et al.,* 2000). Whole-mount staining for β-galactosidase activity at E15 confirmed mosaic expression of TBX5/β-galactosidase mRNA throughout all cardiac chambers (Figs. 4a–4d), and anti-TBX5 immunohistochemistry confirmed rhTBX5 isoform expression by cardiomyocytes exhibiting β-galactosidase activity (Fig. 5). Although a minority of cardiomyocytes expressed rhTBX5 isoforms, significant effects on overall cardiac morphology and size were noted (Figs. 4a–4d). Chick hearts infected with wt-TBX5 retrovirus were approximately 15% smaller than controls (Table 1). Overexpression of ΔASN198FSter-TBX5, which, like wt-TBX5, inhibited proliferation *in vitro,* resulted in similarly small hearts, while overexpression of Gly80Arg-TBX5, an isoform that did not alter proliferation *in vitro,* had no effect on heart size. TUNEL assay demonstrated no evidence of increased apoptosis in any of the TBX5 isoform transgenic chick hearts.

Microscopic analyses suggested further consequences of TBX5 overexpression (Figs. 4e–4p). Overexpression of both wt-TBX5 and ΔASN198FSter-TBX5 produced marked decreases in left and right ventricular trabeculation compared with controls, while overexpression of Gly80Arg-TBX5 did not modify trabeculation (Figs. 4e–4l). Patchy thinning of both atrial walls was also noted in hearts infected with wt-TBX5-CXIZ and ΔASN198FSter-TBX5-CXIZ, but not with Gly80Arg-TBX5-CXIZ (Figs. 4m–4p). Just as the Gly80Arg mutation blocks TBX5-mediated inhibition of chick cardiac trabeculation, humans who are heterozygous for Gly80Arg-TBX5 exhibit abnormal isomerism with markedly increased ventricular trabeculation even in the absence of septation defects (Basson *et al.,* 1994, 1999; Gall *et al.,* 1966). Morphologic changes of the ventricles as a consequence of TBX5 overexpression in the developing chick heart were not associated with abnormal chamber specification. Immunohistochemical studies (Fig. 6) to localize atrial myosin heavy chain demonstrated that its expression remained restricted to the atria in E15 chick hearts and absent from the ventricles in hearts infected with wt-TBX5-CXIZ.

Ventricular trabeculation during cardiogenesis has been

FIG. 4. Retroviral-mediated overexpression of wild-type and mutant TBX5 in embryonic chick hearts. Tubular hearts of HH stage 17–18 chicks were microinjected with CXIZ retrovirus with or without various TBX5 isoforms. Chicks were sacrificed at E15, and the hearts were fixed, stained for β-galactosidase activity, and processed for light microscopy. Whole mounts (a–d) and histological sections (e–p) are shown of hearts infected with (a,e,i,m) CXIZ alone, (b,f,j,n) wt-TBX5-CXIZ, (c,g,k,o) ΔAsn198FSter-TBX5-CXIZ, and (d,h,l,p) Gly80Arg-TBX5-CXIZ. (a–d) Analysis of whole mounts reveals mosaic expression of the transgene; insert images show transmural mosaicism in representative transverse sections through the left ventricular free wall. Gross anatomical analyses also demonstrate a decrease in overall size (see Table 1) in hearts infected with wt-TBX5 and ΔAsn198FSter-TBX5 retroviruses. [Bar (a) for whole-mount images = 1 mm.] (e–p) Representative microscopic images of these genetically manipulated hearts from (e–h) the mid-left ventricular free wall, (i–l) the mid-right ventricular free wall; and (m–p) the right atrium are shown. These studies demonstrate failed or rudimentary ventricular trabeculation in hearts which overexpress wt-TBX5 (f,j) and ΔAsn198FSter-TBX5 (g,k) compared with normal ventricular trabeculation (large arrows) in control CXIZ-infected hearts (e,i) and Gly80Arg-TBX5 overexpressing hearts (h,l). Patchy thinning (small arrows) of the atrial walls is also observed in hearts which overexpress wt-TBX5 (n) and ΔAsn198FSter-TBX5 (o) compared with control CXIZ infected hearts (m) and Gly80Arg-TBX5 overexpressing hearts (p). [Bar (e) for microscopic images = 250 μm.]

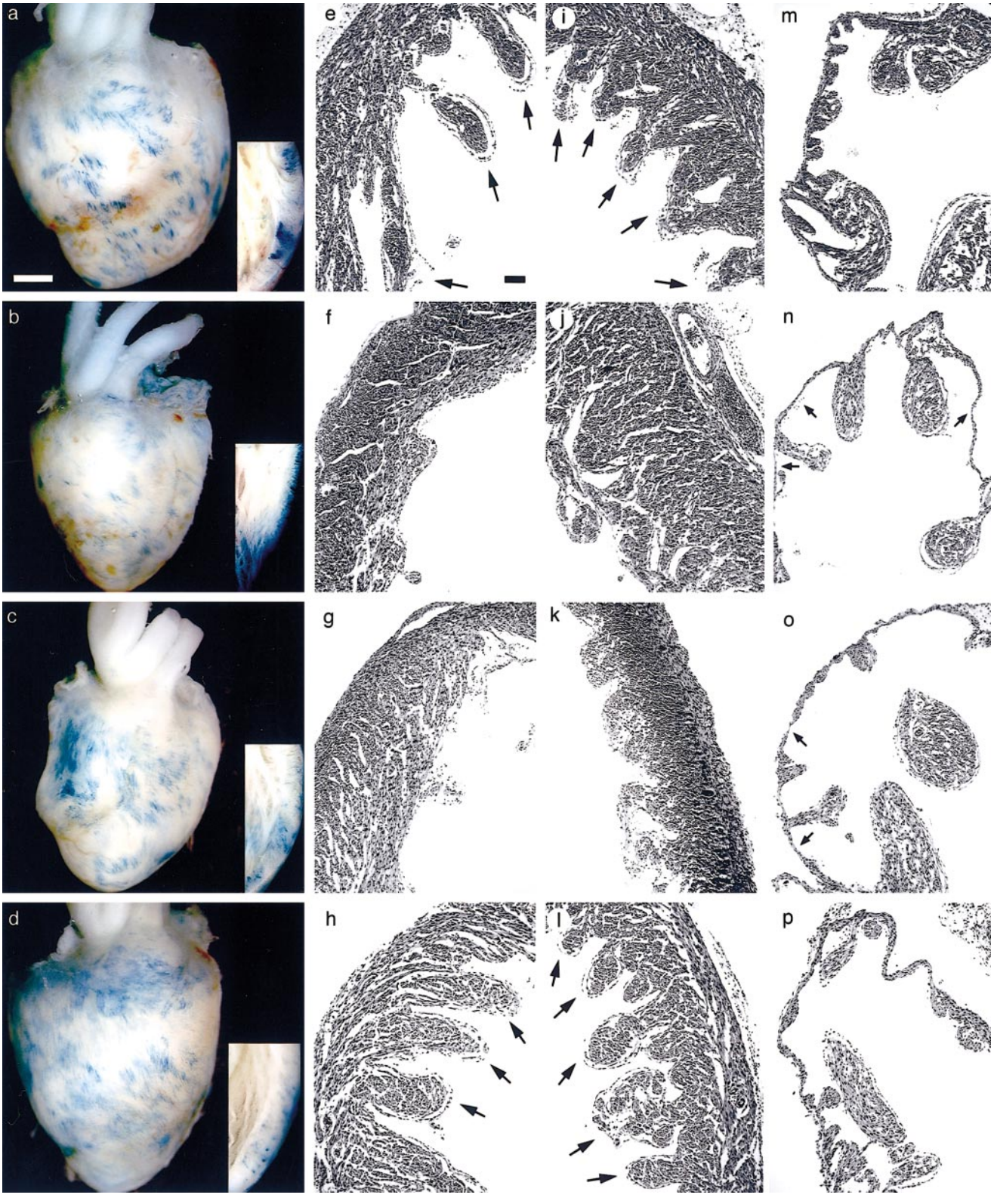

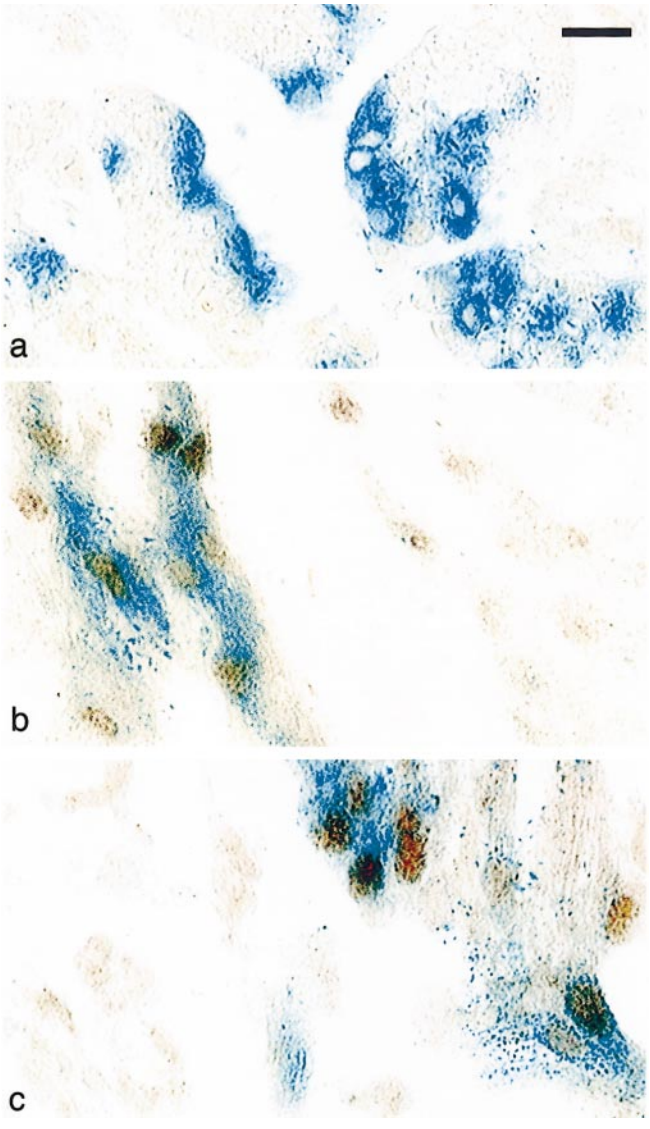

FIG. 5. Immunohistochemical detection of retroviral-mediated rhTBX5 overexpression *in ovo*. Embryonic chick hearts infected with CXIZ retrovirus alone (a), wt-TBX5-CXIZ (b), or Gly80Arg-TBX5-CXIZ were prepared for histology at E15 as in Fig. 3. Five micron sections were immunostained for β-galactosidase activity (blue) and anti-TBX5 (brown). These studies confirmed nuclear expression of rhTBX5 in cardiomyocytes infected by retrovirus and thus exhibiting cytoplasmic β-galactosidase activity.

associated with cardiomyocyte proliferation (Sedmera *et al.*, 2000). Ribozyme antagonism of the mitogen neuregulin-1 (Zhao and Lemke, 1998) and overexpression of the growth arrest protein Gax (Fisher *et al.*, 1997) both decrease cardiomyocyte proliferation with consequent failure of trabeculation. Given our observations that TBX5 inhibits MEQC proliferation *in vitro* and that TBX5 overexpression *in vivo* yields impaired heart growth with decreased ventricular trabeculation, we hypothesized that TBX5 might alter myocardial cell proliferation *in vivo*. To evaluate chick cardiomyocyte proliferation *in vivo*, we immunohistochemically assessed cardiomyocyte synthesis of proliferating cell nuclear antigen (PCNA). The fraction of PCNA-positive cells (Fig. 7) was reduced by 40 and 50% among cardiomyocytes that overexpressed wt-TBX5 and ΔASN198FSter-TBX5, respectively, compared with cardiomyocytes infected with CXIZ alone. Infection with Gly80Arg-TBX5 had no significant effect on PCNA positivity. Remarkably, in all genetically manipulated chick hearts, cardiomyocytes in trabeculae without evidence of retroviral infection exhibited the same degree of PCNA positivity as those in adjacent trabeculae which did express rhTBX5 isoforms (Fig. 7). Thus, the capacity of TBX5 to inhibit cell proliferation *in vivo* as well as *in vitro* is not cell autonomous, and our findings suggest that TBX5 transcriptional regulation of other genes contributes to paracrine signaling among cardiac cells during development.

TBX5 Expression during Human Organogenesis

The ability of TBX5 to inhibit cell proliferation *in vitro* and during chick cardiogenesis prompted us to analyze the relationship between cell proliferation and TBX5 expression during human organogenesis. TBX5 expression patterns during human embryogenesis were compared with expression patterns of two markers of cell proliferation, PCNA and Ki-67, in 10 human embryos of 10–15 weeks of gestation. Immunohistochemical analyses of embryonic human heart, limb, and eye (Fig. 8) revealed that regions of developing tissue which showed significant cellular proliferation, marked by either PCNA (not shown) or Ki-67 staining, exhibited minimal staining for TBX5 and vice versa. TBX5 expression in the heart, as previously described (Chapman *et al.*, 1996; Li *et al.*, 1997; Bruneau *et al.*, 1999; Hatcher *et al.*, 2000), was highest in the atria and lowest in the ventricular myocardium (Figs. 8a and 8c), while cell proliferation was highest in the ventricular myocardium (Fig. 8b). In the embryonic thumb, TBX5 expression was high in developing bone of the distal phalanx (Fig. 8e) and low in musculature surrounding the distal phalanx (Fig. 8g), while cell proliferation showed the opposite pattern (Figs. 8f and 8h). Striking contrast between TBX5 expression and cell proliferation was also observed in the sensory retina of the developing eye where TBX5 was present only in the inner cell layer, not in the outer cell layer (Fig. 8i), to which we, like others (Gao and Hollyfield, 1995), have observed that cell proliferation is restricted (Fig. 8j). Thus, we observed a reciprocal relationship between TBX5 expression and cell proliferation not only in experimental tissue culture and animal models but also in retrospective immunohistochemical analyses of human organogenesis.

TABLE 1
Effects of TBX5 Isoform Overexpression on Chick Heart Development

	CXIZ Control (n = 13)	wt-TBX5 (n = 16)	Gly80Arg-TBX5 (n = 6)	ΔASN198FSter-TBX5 (n = 12)
Heart weight (mg)	70.5 ± 2.5	59.0 ± 1.5[a]	73.5 ± 4.4	58.3 ± 3.0[a]
Tibia length (mm)	1.13 ± 0.04	1.11 ± 0.01	1.12 ± 0.01	1.13 ± 0.03
Heart weight/tibia length (mg/mm)	62.3 ± 2.0	53.2 ± 1.3[a]	64.7 ± 3.3	52.0 ± 2.6[a]

Data are mean ± SEM.
[a] $P < 0.01$ compared with control.

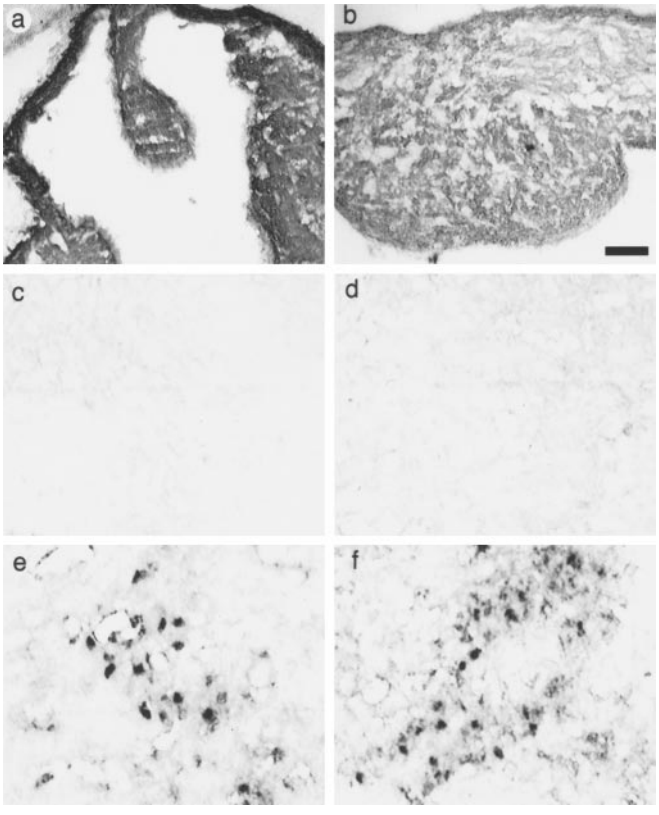

FIG. 6. Atrial myosin heavy-chain expression in TBX5 transgenic chick hearts. Embryonic chick hearts infected with CXIZ retrovirus encoding wild-type TBX5 were prepared for cryosectioning. Parallel sections were immunostained for atrial myosin heavy chain with AMHC1 (a–d) or for rhTBX5 with affinity-purified anti-TBX5 (e,f). AMHC1 staining is shown in (a) right atrium, (b) left atrium, (c) right ventricle, and (d) left ventricle. Parallel ventricular regions to those shown in c and d are shown in e and f with immunostaining for TBX5 which exhibits predominant nuclear localization. AMHC1 staining was restricted to the right (a) and left (b) atria and was absent from the right (c) and left (d) ventricles even in regions where rhTBX5 is expressed at high levels (e,f). [Bar = 50 μm (a,b) or 25 μm (c–f).]

DISCUSSION

In this report, we have demonstrated that TBX5 has a profound inhibitory effect on cell proliferation *in vitro*. Mosaic overexpression of TBX5 *in vivo* during chick cardiogenesis resulted in impaired cardiac morphogenesis which was associated with inhibition of cardiomyocyte proliferation. TBX5 inhibition of cell proliferation *in vitro* and *in vivo* was abrogated by the Gly80Arg TBX5 missense mutation at the 5′ end of the TBX5 T-box but was not altered by deletion of the 3′ end of the T-box. Furthermore, we observed that those cells not overexpressing TBX5 but that were in the same *in vitro* or *in vivo* milieu as cells which were overexpressing TBX5 exhibited similarly decreased proliferation.

Diminished cell numbers during growth in tissue culture can result from inhibition of cell proliferation or cell survival. Our *in vitro* studies of D17s and MEQCs infected with TBX5 retroviruses revealed no evidence of cell necrosis or apoptosis. Similarly, our histological and immunohistochemical analyses of TBX5 transgenic chick hearts with reduced size failed to show any evidence cardiomyocyte necrosis or apoptosis. On the other hand, reduced fractions of PCNA-positive cells in these hearts demonstrate a role for TBX5 in inhibition of cardiomyocyte proliferation. Further investigation of TBX5 antiproliferative activity *in vivo* will determine at what stage TBX5 blocks the cell cycle and the intracellular mediators of this activity.

Other cellular processes and events could potentially contribute to defective organ growth and morphogenesis in TBX5 transgenic chick hearts. Our histologic analyses do not reveal any significant alterations in connective tissue distribution or cardiomyocyte size in these animals. However, we cannot exclude subtle changes in extracellular matrix composition or cell shape as contributors to the decreased heart size in TBX5 transgenic chick hearts. As further investigation establishes the downstream targets of TBX5 that mediate its antiproliferative activity, detailed analyses of extracellular matrix protein expression and cardiomyocyte morphology may be informative.

Abnormal cardiac chamber specification can also alter organogenesis. Just as we observed impaired ventricular

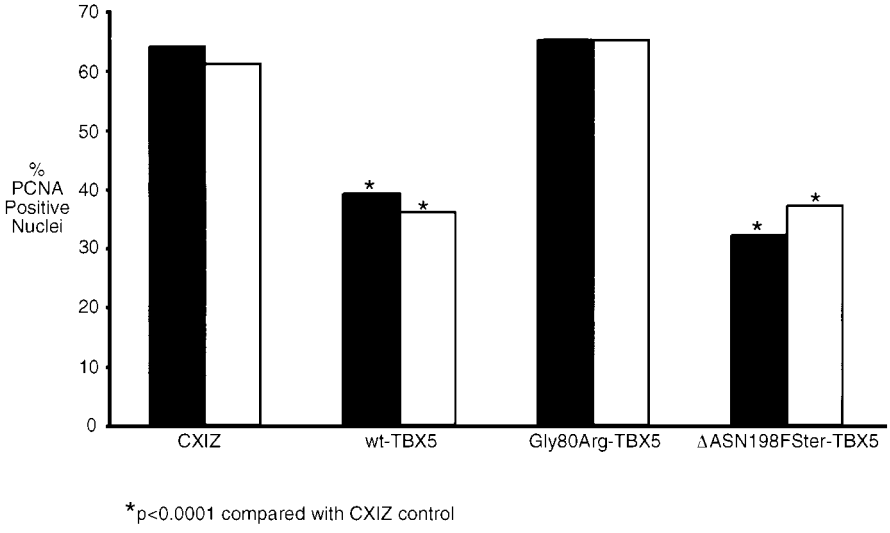

FIG. 7. Effect of TBX5 overexpression on cardiomyocyte proliferation *in vivo*. Embryonic chick hearts were infected with CXIZ retrovirus encoding wild-type and mutant TBX5 isoforms, animals sacrificed at E15, and chick hearts prepared for histology as in Fig. 4. Five micron sections were immunostained with antibodies to β-galactosidase and PCNA. The percentages of PCNA positive nuclei in β-galactosidase-positive cells (solid bars) as well as in β-galactosidase negative cells from uninfected trabeculae (open bars) were calculated. For each TBX5 isoform, more than 500 infected and uninfected cells were counted from six chick hearts. $P < 0.0001$ compared with CXIZ-infected control hearts is denoted (*).

development with decreased trabeculation due to TBX5 overexpression in the chick, Liberatore *et al.* (2000) observed that overexpression of Tbx5 in the murine ventricle resulted in a failure of cardiogenesis. They observed thin-walled ventricular chambers with reduced trabeculation and hypothesized that these abnormalities might involve aberrant chamber specification and atrialization of ventricular myocardium. Immunohistochemical studies in our chick model, though, demonstrate restriction of atrial myosin heavy-chain expression to the atria even in the face of TBX5 isoform overexpression. Thus, our model dissociates cell proliferation from atrial specification. Such dissociation may be a consequence of the timing of TBX5 overexpression intrinsic to the two experimental designs. Although TBX5 overexpression as driven by the β-myosin heavy-chain promoter in the murine model should begin early in development of the primitive heart tube at the 6–8 somite stage (Colbert *et al.*, 1997), TBX5 overexpression in our model commences later, after stages 17–18 of chick development.

We, therefore, suggest that the same altered regulation of cell proliferation that underlies the chick phenotype is operant in the Tbx5 transgenic mouse and participates in the murine cardiogenic defect. It is intriguing to note that in mouse (Bruneau *et al.*, 1999; Liberatore *et al.*, 2000), chick (Bruneau *et al.*, 1999), and humans (Hatcher *et al.*, 2000), TBX5 is expressed in an anterior–posterior gradient during embryogenesis that results in higher levels of atrial expression than ventricular expression. Native TBX5-induced inhibition of cardiomyocyte proliferation may, then, contribute to the atria developing as thin-walled structures rather than thick-walled trabeculated chambers such as the ventricles.

Both *in vitro* and *in vivo*, we observed that nontransgenic cells in the same culture dish or same heart as transgenic TBX5 overexpressing cells exhibited similar inhibition of proliferation. Our observations that infection with the CXIZ retrovirus alone does not alter cell proliferation and that TBX5 antiproliferative activity on both cell populations is abolished by the Gly80Arg missense mutations exclude a nonspecific cytotoxic effect of the constructs used. We, then, propose that TBX5-mediated inhibition of cell proliferation must, at least, include a noncell autonomous component. Such a paracrine effect of TBX5 expression, potentially mediated by either soluble or extracellular matrix bound factors, could contribute TBX5 modulation of overall organ morphology even in the face of local variations in TBX5 expression. Ultimately, identification of cardiac mediators of the TBX5-dependent paracrine signaling that results in regional proliferative arrest will further test this hypothesis.

Why might the Gly80Arg missense mutation of the 5′ end of the T-box diminish the capacity of TBX5 to inhibit cell proliferation whereas deletion of the 3′ end of the T-box does not? On one hand, deletions at either the 5′ or 3′ ends of the *Xenopus* T(Brachyury) T-box alter DNA binding *in vitro* (Kispert and Herrmann, 1993; Kispert *et al.*, 1995), and missense mutation of the TBX5 T-box at Gly80 and Arg237

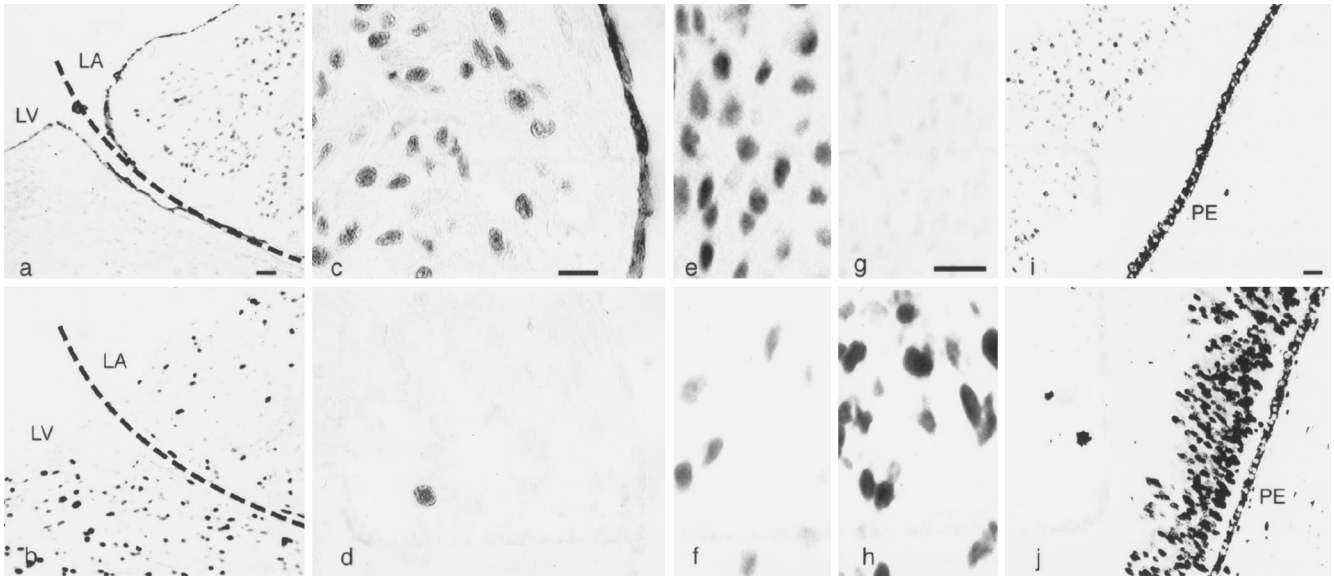

FIG. 8. Expression of TBX5 and a marker of cell proliferation (Ki-67) during human embryogenesis. Heart (a–d), thumb (e–h), and eye (i,j) tissues from 10–15 weeks of gestation of human embryos were immunohistochemically analyzed in parallel tissue sections for expression of TBX5 (a, c, e, g, i) and Ki-67 (b, d, f, h, j). Reciprocal patterns of TBX5 and Ki-67 expression were noted in all tissues. Displayed are representative sections of cardiac tissue from 13.5 (a,b) and 10 week (c,d) embryos, thumb from a 13.5 week embryo (e–h), and eye from an 11 week embryo (i,j). High levels of TBX5 expression (a,c) were observed in the epicardium of the left atria (LA) and left ventricle (LV) as well as the LA myocardium, while high levels of Ki-67 expression (b) were observed only in the LV myocardium. (A dashed line denotes the atrioventricular groove in each section.) Magnified views of the right atrium show similar patterns of TBX5 (c) and Ki-67 expression (d). In the distal phalanx of the thumb, high levels of TBX5 expression were observed only in the bone (e), but not in the surrounding musculature (g) where high levels of Ki-67 expression (h) were observed compared with the bone (f). In the eye, high levels of TBX5 expression (i) were observed only in the inner cell layer of the developing sensory retina, but not in the outer cell layer where high levels of Ki-67 expression were observed (j). Dark coloring of the retinal pigmented epithelium (PE) represents native pigmentation preserved in tissue processing not immunostaining. (Magnification bars = 10 μm.)

both impair T-box/DNA interactions in electromobility shift assays (R. Lin, C. Seidman, J. Seidman, personal communication). On the other hand, crystallographic experiments with the *Xenopus* T(Brachyury) T-box (Müller and Herrmann, 1997) have predicted that the 5′ end of the T-box, including the homologous residue to human TBX5 Gly80 (Basson *et al.*, 1999), encodes a binding domain for target DNA major groove while the 3′ end of the T-box encodes a binding domain for target DNA minor groove. Thus, based on this crystallographic model and our current observations, we hypothesize that TBX5 binding to target DNA major groove is necessary for TBX5-mediated regulation of cell proliferation. However, inhibition of cell proliferation may only be one of many TBX5 contributions to embryogenesis that could require one or both of these putative binding sites.

Finally, we observe significant concordance between the transgenic chick cardiac phenotype and some aspects of the human Holt–Oram cardiac phenotype. Although septation defects are most readily apparent in Holt–Oram patients by noninvasive clinical technology, these defects develop within the broader context of cardiac isomerism defects with abnormal chamber morphogenesis including altered myocardial trabeculation (Gall *et al.*, 1966; Ruzic *et al.*, 1981; Sahn *et al.*, 1981; Hurst *et al.*, 1991; OMIM, 1996; Basson *et al.*, 1999). In our chick studies as well as the Tbx5 transgenic mouse reported by Liberatore *et al.* (2000), TBX5 overexpression disrupts myocardial trabeculation. The Gly80Arg missense mutation which blocks wild-type TBX5 antiproliferative activity in our studies is known to severely compromise human cardiac development (Basson *et al.*, 1999). A hallmark of Holt–Oram syndrome in individuals heterozygous for Gly80Arg-TBX5 is increased right ventricular trabeculation (Gall *et al.*, 1966; Basson *et al.*, 1999). In chick, the overexpression of the Gly80Arg TBX5 mutant has no effect on cardiac development/trabeculation and cardiomyocyte proliferation, and the inhibitory activity of wild-type TBX5 overexpression is not observed. We hypothesize that Holt–Oram patients who are heterozygous for the Gly80Arg-TBX5 mutation may have genetically reduced levels of active wild-type TBX5 which might fail to approximately inhibit cardiomyocyte proliferation during ventricular development and thus result in the increased trabeculation. Yang *et al.'s* (2000) recent identification of

additional TBX5 missense mutations at the 5′ end of the T-box that have cardiovascular consequences in Chinese Holt–Oram patients similar to Gly80Arg-TBX5 will now permit additional evaluation of the potential contribution of this T-box domain to heart development.

The relevance of TBX5's antiproliferative effects to development of other organs besides the heart remains to be determined. Several investigators (Rodriguez-Esteban *et al.*, 1999; Takeuchi *et al.*, 1999; Koshiba-Takeuchi *et al.*, 2000) have used overexpression and misexpression of chick Tbx5 to study organogenesis. During limb outgrowth, chick Tbx5 may participate in a feedback loop with BMP, WNT, and FGF isoforms that regulate proliferation (Rodriguez-Esteban *et al.*, 1999; Takeuchi *et al.*, 1999). Tbx5 may also modify proliferative responses in the developing chick eye where misexpression of chick Tbx5 alters retinotectum axonal projections (Koshiba-Takeuchi *et al.*, 2000). Our survey of available human embryonic tissue shows that TBX5 expression is inversely related to expression of nuclear proliferating antigens in the limb and eye as well as in the heart during human embryogenesis. These observations are consistent with a role for T-box transcription factor regulation of proliferative responses during ontogeny of these other organ systems. Identification of genes regulated by TBX5 will ultimately define molecular genetic pathways that mediate paracrine regulation of cell proliferation during vertebrate organogenesis.

ACKNOWLEDGMENTS

Dr. Basson is supported by NIH-HL03468, NIH-HL61785, the Edward Mallinckrodt, Jr. Foundation, and the March of Dimes Birth Defects Foundation and Dr. Hatcher is supported by a NHLBI Minority Postdoctoral Supplement. The authors are grateful for technical assistance by K. Cedeno-Baier, B. Furman, and E. Hartley, and for advice and comments by Dr. Donald A. Fischman.

REFERENCES

Basson, C. T., Cowley, G. S., Solomon, S. D., Weissman, B., Poznanski, A. K., Traill, T. A., Seidman, J. G., and Seidman, C. E. (1994). The clinical and genetic spectrum of the Holt-Oram syndrome (heart-hand syndrome). *N. Engl. J. Med.* **330,** 885–891.

Basson, C. T., Bachinsky, D. R., Lin, R. C., Levi, T., Elkins, J. A., Soults, J., Grayzel, D., Kroumpouzou, E., Traill, T. A., LeBlanc-Straceski, J., Renault, B., Kucherlapati, R., Seidman, J. G., and Seidman, C. E. (1997). Mutations in human *TBX5* cause limb and cardiac malformation in Holt-Oram syndrome. *Nat. Genet.* **15,** 30–35.

Basson, C. T., Huang, T., Lin, R. C., Bachinsky, D. R., Weremowicz, S., Vaglio, A., Bruzzone, R., Quadrelli, R., Lerone, M., Romeo, G., Silengo, M., Pereira, A., Krieger, J., Mesquita, S. F., Kamisago, M., Morton, C. C., Pierpont, M. E. M., Müller, C. W., Seidman, J. G., and Seidman, C. E. (1999). Different *TBX5* interactions in heart and limb defined by Holt-Oram syndrome mutations. *Proc. Natl. Acad. Sci. USA* **96,** 2919–2924.

Bruneau, B. G., Logan, M., Davis, N., Levi, T., Tabin, C. J., Seidman, J. G., and Seidman, C. E. (1999). Chamber-specific cardiac expression of *TBX5* and heart disease in Holt-Oram syndrome. *Dev. Biol.* **211,** 100–108.

Chapman, D. L., Garvey, N., Hancock, S., Alexiou, M., Agulnik, S. I., Gibson-Brown, J. J., Cebra-Thomas, J., Bollag, R. J., Silver, L. M., and Papaioannou, V. E. (1996). Expression of the T-box family genes, *Tbx1-Tbx5*, during early mouse development. *Dev. Dyn.* **206,** 370–390.

Colbert, M. C., Hall, D. G., Kimball, T. R., Witt, S. A., Lorenz, J. N., Kirby, M. L., Hewett, T. E., Klevitsky, R., and Robbins, J. (1997). Cardiac compartment-specific overexpression of a modified retinoic acid receptor produced dilated cardiomyopathy and congestive heart failure in transgenic mice. *J. Clin. Invest.* **100,** 1958–1968.

Dixon, J. W., Costa, T., and Teshima, I. E. (1993). Mosaicism for duplication 12q (12q13–q24.2) in a dysmorophic male infant. *J. Med. Genet.* **30,** 70–72.

Fisher, S. A., Siwik, E., Branellec, D., Walsh, K., and Watanabe, M. (1997). Forced expression of the homeodomain protein Gax inhibits cardiomyocyte proliferation and perturbs heart morphogenesis. *Development* **124,** 4405–4413.

Gall, J. C., Stern, A. M., Cohen, M. M., Adams, M. S., and Davidson, R. T. (1966). Holt-Oram syndrome: Clinical and genetic study of a large family. *Am. J. Hum. Genet.* **18,** 187–200.

Gao, H., and Hollyfield, J. G. (1995). Basic fibroblast growth factor in retinal development: Differential levels of bFGF expression and content in normal and retinal degeneration (*rd*) mutant mice. *Dev. Biol.* **169,** 168–184.

Hamburger, V., and Hamilton, H. L. (1951). A series of normal stages in the development of the chick embryo. *J. Morph.* **88,** 49–92.

Hatcher, C. J., and Basson, C. T. (2000). Holt-Oram syndrome and the TBX5 transcription factor in cardiogenesis. *In* "Molecular Genetics of Cardiac Electrophysiology" (C. I. Berul and J. A. Towbin, Eds.), pp. 297–315. Kluwer Academic, Norwell, MA.

Hatcher, C. J., Goldstein, M. M., Mah, C. S., Delia, C. S., and Basson, C. T. (2000). Identification and localization of TBX5 transcription factor in human cardiac morphogenesis. *Dev. Dyn.* **219,** 90–95.

Herrmann, B. G., and Kispert, A. (1994). The T genes in embryogenesis. *Trends Genet.* **10,** 280–286.

Horb, M. E., and Thomsen, G. H. (1999). Tbx5 is essential for heart development. *Development* **126,** 1739–1751.

Hurst, J. A., Hall, C. M., and Baraitser, M. (1991). The Holt-Oram syndrome. *J. Med. Genet.* **28,** 406–410.

Jaffredo, T., Chestier, A., Bachnou, N., and Dieterlen-Lièvre, F. (1991). MC29-Immortalized clonal avian heart cell lines can partially differentiate *in vitro*. *Exp. Cell Res.* **192,** 481–491.

Kispert, A., and Herrmann, B. G. (1993). The *Brachyury* gene encodes a novel DNA binding domain. *EMBO J.* **12,** 3211–3220.

Kispert, A., Koschorz, B., and Herrmann, B. G. (1995). The T protein encoded by *Brachyury* is a tissue-specific transcription factor. *EMBO J.* **14,** 4763–4772.

Koshiba-Takeuchi, K., Takeuchi, J. K., Matsumoto, K., Momose, T., Uno, K., Hoepker, V., Ogura, K., Takahashi, N., Nakamura,

H., Yasuda, K., and Ogura, T. (2000). Tbx5 and the retinotectum projection. *Science* **287,** 134–137.

Li, Q. Y., Newbury-Ecob, R. A., Terrett, J. A., Wilson, D. I., Curtis, A. R., Yi, C. H., Gebuhr, T., Bullen, P. J., Robson, S. C., Strachan, T., Bonnet, D., Lyonnet, S., Young, I. D., Raeburn, J. A., Buckler, A. J., Law, D. J., and Brook, J. D. (1997). Holt-Oram syndrome is caused by mutations in TBX5, a member of the Brachyury (T) gene family. *Nat. Genet.* **15,** 21–29.

Liberatore, C. M., Searcy-Schrick, R. D., and Yutzey, K. E. (2000). Ventricular expression of *tbx5* inhibits normal heart chamber development. *Dev. Biol.* **223,** 169–180.

McCorquodale, M. M., Rolf, J., Ruppert, E. S., Kurczynski, T. W., and Kolacki, P. (1986). Duplication (12q) syndrome in female cousins, resulting from maternal (11;12)(p15.5;q24.2) translocations. *Am. J. Med. Genet.* **24,** 613–622.

Mealy, K. L., Barhoumi, R., Rogers, K., and Kochevar, D. T. (1998). Doxorubicin induced expression of p-glycoprotein in a canine osteosarcoma cell line. *Cancer Lett.* **126,** 187–192.

Melnyk, A. R., Weiss, L., Van Dyke, D. L., and Jarvi, P. (1981). Malformation syndrome of duplication 12q24.1-qter. *Am. J. Med. Genet.* **10,** 357–365.

Mikawa, T., Borisov, A., Brown, A. M. C., and Fischman, D. A. (1992a). Clonal analysis of cardiac morphogenesis in the chicken embryo using a replication-defective retrovirus. I. Formation of the ventricular myocardium. *Dev. Dyn.* **193,** 11–23.

Mikawa, T., Cohen-Gould, L., and Fischman, D. A. (1992b). Clonal analysis of cardiac morphogenesis in the chicken embryos using a replication-defective retrovirus. III. Polyclonal origin of adjacent ventricular myocytes. *Dev. Dyn.* **195,** 133–141.

Mikawa, T. (1995). Retroviral targeting of FGF and FGFR in cardiomyocytes and coronary vascular cells during heart development. *Ann. N.Y. Acad. Sci.* **752,** 506–516.

Mima, T., Ueno, H., Fischman, D. A., Williams, L. T., and Mikawa, T. (1995). FGF-receptor is required for *in vivo* cardiac myocyte proliferation at early embryonic stages of heart development. *Proc. Natl. Acad. Sci. USA* **92,** 467–471.

Müller, C. W., and Herrmann, B. G. (1997). Crystallographic structure of the T-domain-DNA complex of the *Brachyury* transcription factor. *Nature* **389,** 884–888.

Online Mendelian Inheritance in Man, OMIM™. Center for Medical Genetics, Johns Hopkins University (Baltimore, MD) and National Center for Biotechnology Information, National Library of Medicine (Bethesda, MD). (1996). Worldwide Web URL: http://www.ncbi.nlm.nih.gov/omim/

Rodriguez-Esteban, C., Tsukui, T., Yonei, S., Magallon, J., Tamura, K., Belmonte, J. C. I. (1999). The T-box genes *Tbx4* and *Tbx5* regulate limb outgrowth and identity. *Nature* **398,** 814–818.

Ruzic, B., Bosnar, B., and Beleznay, O. (1981). Ein seltener herzfehler als symptom des Holt-Oram-Syndroms. *Radiologe* **21,** 296–299.

Sahn, D. J., Goldberg, S. J., Allen, H. D., and Canale, J. M. (1981). Cross-sectional echocardiographic imaging of supracardiac total anomalous pulmonary venous drainage to a vertical vein in a patient with Holt-Oram syndrome. *Chest* **21,** 296–299.

Sanders, E., Moorman, A. F. M., and Los, J. A. (1984). The local expression of adult chicken heart myosins during development. I. The three days embryonic chicken heart. *Anat. Embryol.* **169,** 185–191.

Sedmera, D., Pexieder, T., Vuillemin, M., Thompson, R. P., and Anderson, R. H. (2000). Developmental patterning of the myocardium. *Anat. Rec.* **258,** 319–337.

Shoieb, A. M., Hahn, K. A., Barnhill, M. A. (1998). An in vivo/in vitro experimental model system for the study of human osteosarcoma: canine osteosarcoma cells (COS31) which retain osteoblastic and metastatic properties in nude mice. *In Vivo* **12,** 463–472.

Simon, H.-G., Kittappa, R., Khan, P. A., Tsilfidis, C., Liversage, R. A., Oppenheimer, S. (1997). A novel family of T-box genes in urodele amphibian limb development and regeneration: Candidate genes involved in vertebrate forelimb/hindlimb patterning. *Development* **124,** 1355–1366.

Takebayashi-Suzuki, K., Yanagisawa, M., Gourdie, R. G., Kanzawa, N., and Mikawa, T. (2000). In vivo induction of cardiac purkinje fiber differentiation by co-expression of preproendothelin-1 and endothelin converting enzyme-1. *Development* **127,** 3523–3532.

Takeuchi, J. K., Koshiba-Takeuchi, K., Matsumoto, K., Vogel-Hopker, A., Naitoh-Matsui, M., Ogura, K., Takahashi, N., Yasuda, K., and Ogura, T. (1999). *Tbx5* and *Tbx4* genes determine the wing/leg identity of limb buds. *Nature* **398,** 810–814.

Wei, Y., and Mikawa, T. (2000). Formation of the avian primitive streak from spatially restricted blastoderm: Evidence for polarized cell division in the elongating streak. *Development* **127,** 87–96.

Yang, J., Hu, D., Xia, J., Yang, Y., Ying, B., Hu, J., and Zhou, Z. (2000). Three novel TBX5 mutations in Chinese patients with Holt-Oram syndrome. *Am. J. Med. Genet.* **92,** 237–240.

Zhao, J. J., and Lemke, G. (1998). Selective disruption of neuregulin-1 function in vertebrate embryos using riboszyme-tRNA transgenes. *Development* **125,** 1899–1907.

Received for publication July 20, 2000
Accepted December 1, 2000
Published online January 19, 2001